Thermal History Paint Under High Subsonic Flow

Wit Strycniewicz[1], Tomasz Kwiatkowski[1], Izabela Kamińska[2],
Michał Chojnacki[2], Krzysztof Fronc[2]

[1] Łukasiewicz Research Network – Institute of Aviation, al. Krakowska 110/114, 02-256 Warsaw, Poland
[2]Institute of Physics Polish Academy of Sciences, al. Lotników 32/46, Warsaw 02-668, Poland

Abstract

The paper studies the influence of aerodynamic stress on thermal history paint measurement results. The main objective of work is to investigate the performance of sensor coatings exposed to high-speed flows. For this purpose, specimens covered with thermal history paint has been simultaneously exposed to high thermal loads and high subsonic airflow. The test stand included an open tests section Joule furnace for handling the specimens covered with investigated paint, a subsonic nozzle, and a set-up of conventional non-contact temperature measurement devices: two pyrometers and high-resolution IR-camera. Inconel specimen covered by thermal history paint was exposed to Mach 0.6 flow. The specimen was heated by Joule effect to maximum temperature 1000 °C. Off-line measurements of the maximum temperature surface distribution with thermal history paint confirmed the on-line measurement results with IR camera and pyrometers. The results might be useful for jet engine and turbomachinery R&D development teams.

Keywords: thermal history sensing, heat and mass transfer, luminescent thermometry

1. General Introduction

Recent years, off-line determinant of thermal history has been used in many aerospace applications such as jet engine development [1][2] and power generation . The principle behind this technology is to use permanent changes of fluorescence characteristics caused by thermal events in luminophore materials. This technique allows to measure maximum temperature distribution on the investigated component at room temperature after cooling of the object. Although number of applications of Thermal History Coatings and Thermal History Paints in field of aerospace engineering is growing [3], there is a lack of detailed data on the performance of THC under high aerodynamic shear caused by high subsonic flow. The sensor coatings especially in form of paints exposed to high-speed flow inside jet engine might be prone to degradation. Recent research on thermal profiling of turbocharger compressor wheels using phosphorescence thermal history coatings [4] reviled degradation of the Thermal History Paint layer due to mechanical abrasion or contact with particles. In jet engine testing, one can expect degradation of THP coatings on surfaces exposed to combustion gases due to shear stress, spallation. Thermal profiling in non-dedicated jet engine combustor testing proved robustness of Thermal History Coating for elongated time including muliti-cyclicing [5]. In [6] THP exhibited good durability during tests of cooled radial turbine wheels in a hot gas rig. Nevertheless, dedicated studies on performance of Thermal History Paints exposed to high-speed flows are still lacking. In our paper we have investigated the influence on aerodynamic shear stress on THP measurements in dedicated experimental study aimed to isolate potential reason of paint layer degradation in jet engine testing.

2. Materials and methods

2.1 Joule Furnace

To control the temperature a concept of Joule furnace was adopted in which the specimen itself would be the heating element. Temperature gradients were obtained by flow of high amperage DC current through a variable cross-section of the specimen. The control and measurement system of the Joule furnace enables precise control of the heating time profile and registration of measurement signals. The heating process is controlled via a control application prepared in the LabVIEW environment. To compensate the thermal expansion of the specimen the electrodes was placed on a system of linear bearings. Additionally, the electrodes were electrically isolated with ceramics plates form top and bottom due to large amperage (up to 1000 A). The 3D CAD model of the specimen heating system is presented in Figure 1. The design and thermal properties of materials used for Joule furnace construction allow for heating the specimens for temperature up to 1300 °C.

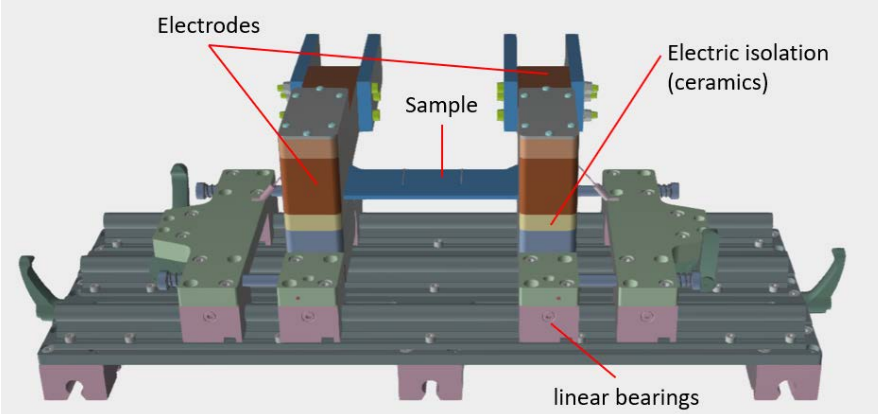

Figure 1 3D CAD model of the Joule furnace

The furnace was installed in front of subsonic nozzle, so the specimen was exposed to high-speed jet. The specimen was placed in the potential cone of the jet. The nozzle was connected to air supply installation allowing to derive up to 2 $kg \cdot s^{-1}$ of pressurized air. Precise control over air mass flow rate was provided with use of automated control system. Mach 0.6 flow was achieved by use PID controlled valve system connected to high pressure reservoir. The pressurized installation is equipped with particle filters in order to provided clean air to the nozzle in test section.

To ensure good flow uniformity, the nozzle's shape was optimized using Computational Fluid Dynamics (CFD) methods. The inlet diameter of the nozzle was 150 mm and the outlet diameter was assumed to be 60 mm. The aim of the optimization was to achieve the widest possible distribution of constant speed equal to Ma = 0.6 in the potential cone of jet. The nozzle optimization was carried out in 2D axisymmetric domains. An optimization loop was defined, beginning with the definition of control points that determined the spline encompassing the nozzle's shape. The spline was generated in ICEM software, and simultaneously, the computational mesh utilizing 2D blocks was created. The computational grids prepared in this way were loaded into the ANSYS Fluent computational solver, in which numerical calculations of the flow were performed. As a result of optimization, the optimal shape of the nozzle was found, which ensured a wide jet of constant speed. The figure below shows the distribution of the Mach number around the channel after optimization. The goal was to achieve a wide distribution of constant velocity in the cross-section X = 0.26 m. The results of CFD calculations on final nozzle geometry is presented in Figure 2.

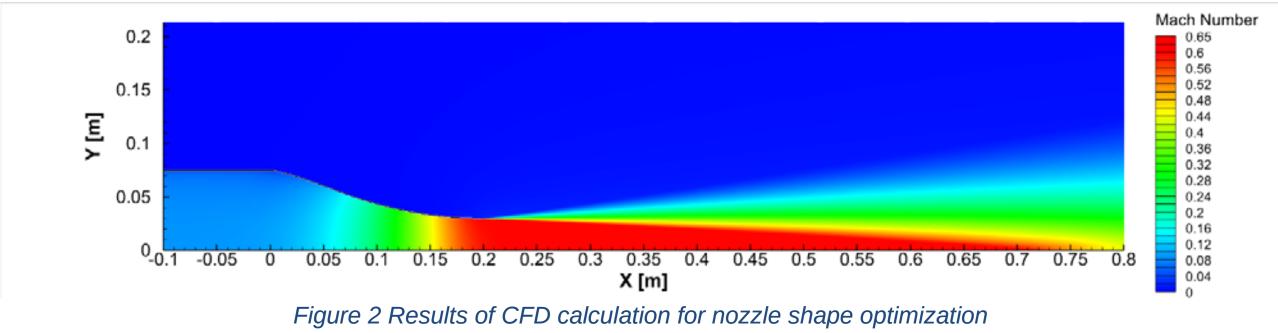

Figure 2 Results of CFD calculation for nozzle shape optimization

2.2 Temperature measurements

To compare the measurement results using temperature history coatings with the measurement results using conventional methods, a measurement system consisting of the following elements included: Optris CTLaser 2MH-CF4 single-color pyrometer, SENSORTHERM METIS M3 two-color pyrometer, FLIR T1020 thermal imaging camera and NI measurement card with a set of K-type thermocouples (TC).

Table 1 Measurement instruments used during heating of the specimen with measurements uncertainties

Type of instrument	Name	Measurement Uncertainty
Two-colour pyrometer	SENSORTHERM METIS M3	0.04% reading + 1 K
One-colour pyrometer	Optris CTLaser 2MH-CF4	0.3% reading + 2 K
IR Camera	FLIR T1020	2°C

In silent conditions testing without the flow the results of thermocouple temperature measurements was lower by more than 20% comparing to other non-contact measurement techniques. The difference was attributed to not perfect contact between the thermocouple measurement junction and specimen surface. In result TC measurements results was not considered in further analysis. Furthermore, thermocouples mounted on the surface of specimen significantly disturbs the flow in proximity of thin specimen covered with THP. The complete experimental setup is presented in Figure 3.

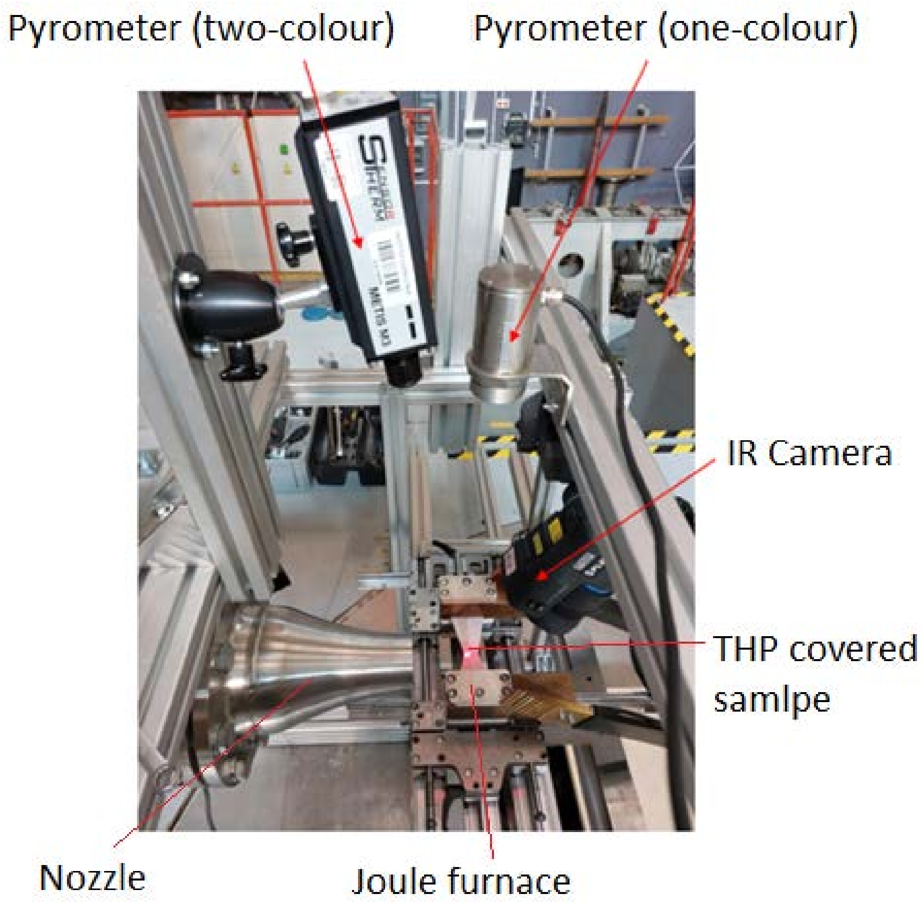

Figure 3 – View of test stand for investigations of thermal history paint under high subsonic flow

2.3 Thermal history paint

The paint was formulated in-house by mixing gadolinium oxide nanopowder doped with rare earth ions [7] with $MgSiO_2$ based commercial binder. The paint was deposed by miniature spray-gun with 0,8 mm nozzle and air supply pressure of 7 bars. One side of butterfly specimen made of Inconel-HX alloy was covered. A “butterfly” shaped specimen was cut with use of EDM wire method.

The luminescence signal of the paint was measured after the tests on specimens at room temperature with use of 980 nm laser and spectrofluorometer. The measurement head was placed on 3D cartesian manipulator for precise data collection (Figure 4). Linear actuators of the traversing system allow to achieve precision of less than 0,5 mm in measurement head placement for pointwise scanning of luminesce signal.

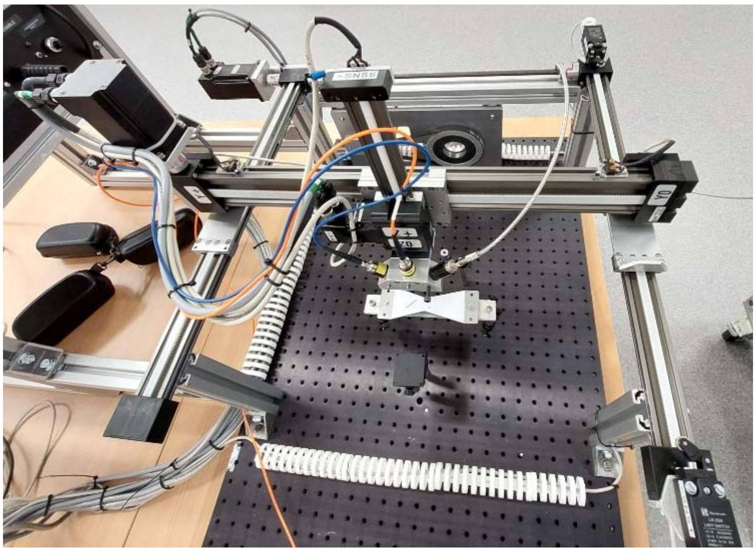

Figure 4 – 3D cartesian manipulator with measurement head over the investigated specimen

The principle of operation of temperature history coatings is to permanently change the luminescent characteristics (like luminescence spectrum or luminescence decay time). Figure 5 show the results of spectrometric measurements of coatings heated at different temperatures for the Inconel HX base material. Both the signal level and luminescence intensity changes are visible. These changes are distinctive for temperature and the ratio of the intensity integrated for wavelength 550 - 600 nm and 670 - 720 nm is used for preparation of calibration curves. The maximum temperature of cooled specimens is derived from luminescence signal with use of paint's calibration data.

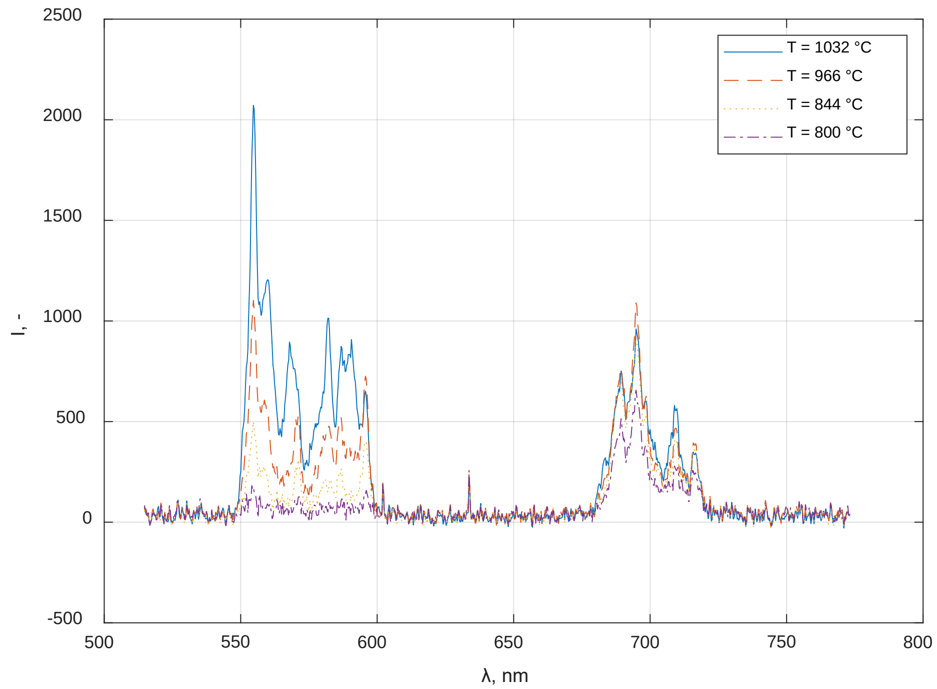

Figure 5 Luminescence spectrum of THP captured on calibration specimens

3. Results

Figure 6 shows results of simultaneous Joule heating and intensive cooling of specimen by forced convection of flow at Mach 0.6. The resulted temperature of paint covered side of the specimen was simultaneously measured with use of IR camera and two pyrometers. Unpainted surface of the specimen has changed color typically for Inconel with characteristic darkening in temperatures above 500 °C. The same pattern surface temperature distribution, resulted from simultaneous heating and exposition to Mach 0.6 flow, can by observed both on Figure 6 and Figure 7.

Figure 6 View of uncovered cold specimen after heating to 1000 °C and exposing to Mach 0.6 flow

IR camera measurement result is presented in Figure 7. The black spot close to specimen minimum cross-section is a place without paint cover.

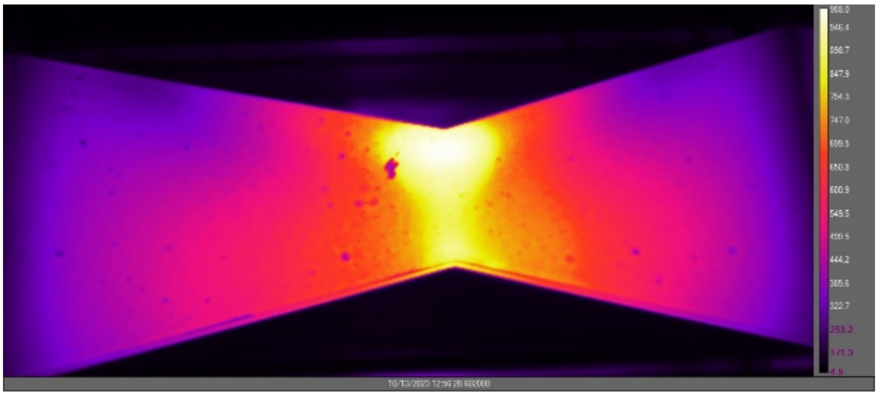

Figure 7 IR thermogram from experiments – maximum temperature field of thermal history paint covered specimen.

Figure 8 shows maximum temperature field determined with thermal history paint after cooling of the specimen to room temperature. Temperature contours was obtained by point-by-point scanning with resolution of 1 mm on a cartesian grid. The 2D temperature map is presented as 3D plot to amplify the maximum temperature distribution. No interpolation was performed on the results presented in Figure 8. The presented results do not reveal any spots with significant losses of paint's luminescence signal.

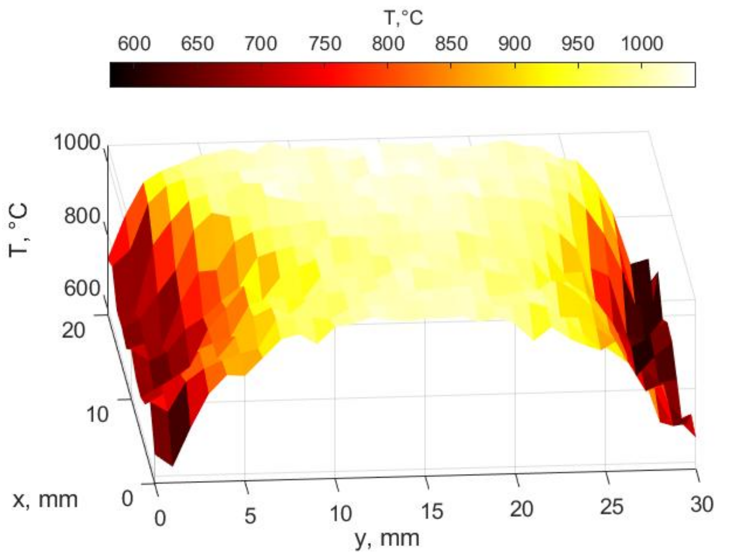

Figure 8 Maximum temperature field determined by Thermal History Paint,

Results of thermal profiling of sample not exposed to flow performed with use of THP are compared with pyrometric results in Figure 9. Good agreement between THP and pyrometric results was achieved. The THP measurement uncertainty was estimated to less than 10 K for temperatures above 1000 °C. Temperature vales obtained by both techniques match well in all investigated area.

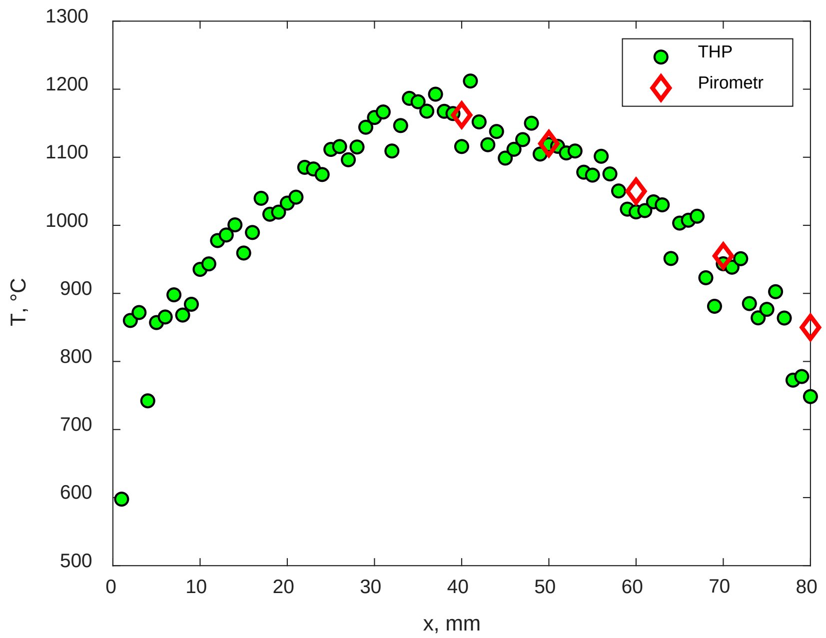

Figure 9 Comparison of thermal profile of the specimen from THP and pyrometry.

4. Conclusions

One can observe that good compatibility between pyrometry and thermal history paint has been achieved. The results provide convincing evidence on the robustness of THP under high subsonic flow conditions. The 2D maximum temperature distribution determined by THP is smooth without any significant discontinuities and no-signal spots. The results indicate that high speed subsonic flow of filtered air does not affect the measurement results. This implies that the paint degradation observed by other research might be caused mostly by paint spallation due to solid particles or reactive. In conclusion we found no major influence of Mach 0.6 flow of pure air on the measurement results.

5. Acknowledgements

This study was supported by the National Centre for Research and Development, Poland, Research Project No POIR.01.01.01-00-0832/19-00.

6. Contact Author Email Address

mailto: wit.stryczniewicz@ilot.lukasiewicz.gov.pl

7. Copyright Statement

References

[1] Feist, J. P., Karmakar Biswas, S. K., Pilgrim, C. C., Sollazzo, P. Y., and Berthier, S. “Off-Line Temperature Profiling Utilizing Phosphorescent Thermal History Paints and Coatings.” *Journal of Turbomachinery*, Vol. 137, No. 10, 2015. https://doi.org/10.1115/1.4030259.

[2] Feist, J. P., Sollazzo, P. Y., Berthier, S., Charnley, B., and Wells, J. “Application of an Industrial Sensor Coating System on a Rolls-Royce Jet Engine for Temperature Detection.” *Journal of Engineering for Gas Turbines and Power*, Vol. 135, No. 1, 2013, pp. 1–9. https://doi.org/10.1115/1.4007370.

[3] Fouliard, Q., Ebrahimi, H., Hernandez, J., Vo, K., Accornero, F., McCay, M., Park, J. S., Almer, J., Ghosh, R., and Raghavan, S. “Stresses within Rare-Earth Doped Yttria-Stabilized Zirconia Thermal

Barrier Coatings from in-Situ Synchrotron X-Ray Diffraction at High Temperatures." *Surface and Coatings Technology*, Vol. 444, 2022. https://doi.org/10.1016/j.surfcoat.2022.128647.

[4] Karagiannopoulos, S., Castillo, D., Rode, M., Araguas-rodríguez, S., and Peral, D. Advanced Thermal Profiling of Turbocharger Compressor Wheels Using. 2022.

[5] Peral, D., Zaid, A., Benninghoven, C., Araguás-Rodríguez, S., Kluß, D., Karagiannopoulos, S., Krewinkel, R., and Feist, J. P. "High-Resolution Thermal Profiling of a Combustor in a Non-Dedicated Test Using Thermal History Coatings." *Journal of Turbomachinery*, Vol. 144, No. 11, 2022. https://doi.org/10.1115/1.4054635.

[6] Pilgrim, C. C., Castillo, D., Araguás-Rodríguez, S., Karagiannopoulos, S., Feist, J. P., Redwood, A., Zhang, Y., Copeland, C., Scobie, J., and Sangan, C. Thermal Profiling of Cooled Radial Turbine Wheel. 2020.

[7] Kamińska, I., Wosztyl, A., Kowalik, P., Sikora, B., Wojciechowski, T., Sobczak, K., Minikayev, R., Zajdel, K., Chojnacki, M., Zaleszczyk, W., Łysiak, K., Paszkowicz, W., Szczytko, J., Frontczak-Baniewicz, M., Stryczniewicz, W., and Fronc, K. "Synthesis and Characterization of Gd 2 O 3 : Er 3+ , Yb 3+ Doped with Mg 2+ , Li + Ions—Effect on the Photoluminescence and Biological Applications." *Nanotechnology*, Vol. 32, No. 24, 2021, p. 245705. https://doi.org/10.1088/1361-6528/abed02.